

Spatial Assessment of Soil Erosion Variability in Kwara State, Nigeria Using RUSLE and GIS

*Ipadeola O.A., Adeniyi F.E., Olatunde G., Yusuf A., Babalola A. & Gbadamosi A.A.

Department of Surveying and Geoinformatics, University of Ilorin, Ilorin

*Corresponding author: ipadeola.ao@unilorin.edu.ng

Received: 14/04/2026

Revised: 29/04/2026

Accepted: 4/05/2026

Soil erosion poses a significant challenge to agricultural productivity and land sustainability in Kwara State, Nigeria. This study assesses the spatial variability of soil erosion risk across the state using the Revised Universal Soil Loss Equation (RUSLE) integrated with Geographic Information Systems (GIS) and remote sensing data. Rainfall erosivity (R-factor) was estimated from 30 years (1992–2022) of mean annual precipitation using an empirical relationship suitable for data-limited environments, while other RUSLE factors (K, LS, C, and P) were derived from soil data, digital elevation models, and satellite-based vegetation indices.

The model outputs were integrated to generate a spatial map of average annual soil loss, which was classified into low, medium, and high erosion risk categories. Results indicate that approximately 73.15% of the study area falls within the low-risk class, 23.04% within the medium-risk class, and 3.81% within the high-risk class, with higher erosion susceptibility observed in areas associated with steeper slopes, sparse vegetation, and intensive land use. Model validation was conducted using a limited number of ground-referenced observations through a confusion matrix approach, yielding an overall accuracy of 93% and a kappa coefficient of 0.87. These metrics indicate good agreement but should be interpreted with consideration of the sample size and spatial coverage of validation data. The findings provide a regional-scale indication of erosion risk patterns and highlight areas where soil conservation measures may be prioritized. However, the results represent model-based estimates of relative erosion susceptibility and should be interpreted cautiously. The study offers a useful baseline for supporting land management planning while underscoring the need for further validation and uncertainty analysis.

Keywords: Soil loss, RUSLE, GIS, Variability, Erosivity, Erodibility.

Introduction

Soil erosion remains a dominant form of land degradation, with direct implications for agricultural productivity, ecosystem stability, and hydrological systems. The removal of topsoil reduces nutrient availability and accelerates sediment delivery to river networks, thereby increasing flood risk and impairing water quality (Panagos *et al.*, 2015; Borrelli *et al.*, 2017). These impacts are particularly pronounced in tropical regions, where high-intensity rainfall and land-use pressures interact to amplify erosion processes.

In sub-Saharan Africa, soil erosion is increasingly linked to the combined effects of climatic variability, fragile soil conditions, and anthropogenic land transformation. In Nigeria, rapid agricultural expansion, deforestation, and poorly managed land-use practices have intensified soil degradation across multiple ecological zones. Empirical evidence suggests that erosion patterns in such environments are spatially heterogeneous, controlled primarily by the interaction of rainfall intensity, topographic gradients, vegetation cover, and soil properties (Tamene & Vlek, 2008). Despite growing research interest, erosion assessments in Nigeria remain largely confined (Alemu *et al.*, 2026; to watershed or local-scale studies, limiting their applicability for broader land-use planning and policy interventions (Anejionu *et al.*, 2013; Thapa, 2020).

The Revised Universal Soil Loss Equation (RUSLE) provides a widely adopted empirical framework for

estimating long-term average soil loss by integrating rainfall erosivity, soil erodibility, topography, vegetation cover, and conservation practices (Renard *et al.*, 2017). When coupled with Geographic Information Systems (GIS) and remote sensing, RUSLE enables spatially distributed modelling of erosion risk across large areas (Ganasri & Ramesh, 2016; Kayet *et al.*, 2018). This integration has proven effective in identifying erosion-prone zones and supporting land management decisions in data-scarce environments.

However, the application of RUSLE at broader spatial scales introduces important methodological challenges. First, the model is empirical and estimates long-term average soil loss, without capturing event-based dynamics such as extreme rainfall or episodic erosion events. Second, its performance in tropical environments is constrained by the limited availability of high-resolution rainfall intensity data required for robust erosivity estimation. Third, RUSLE does not clearly represent gully erosion, channel processes, or sediment deposition, which can contribute significantly to total soil loss in many landscapes (Boardman & Poesen, 2006; Poesen, 2018). These limitations necessitate careful interpretation of model outputs as indicators of relative erosion susceptibility rather than precise quantitative predictions.

In addition, scaling erosion modelling to administrative units such as states requires the integration of multi-source datasets with varying spatial resolutions. While such integration enables

continuous spatial analysis, it introduces uncertainty related to data resampling, parameter generalization, and validation coverage. These factors directly influence the magnitude and spatial distribution of predicted soil loss and must be explicitly acknowledged.

Within this context, there is a need for spatially referenced, regional-scale erosion assessments that provide continuous information on erosion risk while maintaining transparency regarding model assumptions, data limitations, and validation constraints. Such assessments are particularly valuable in data-scarce environments, where model-based approaches support decision-making but must be interpreted cautiously.

This study, therefore, presents a state-wide assessment of the spatial variability of soil erosion risk in Kwara State, Nigeria, using the RUSLE model integrated with GIS and remotely sensed datasets. Unlike previous studies that focus on localized catchments, this research adopts a broader spatial perspective to evaluate relative erosion patterns across the state. The study also incorporates field-based observations for classification validation, while acknowledging the limitations associated with model structure, data availability, and validation scale. The results are intended to provide a regional-scale baseline for identifying erosion-prone areas and supporting targeted land management interventions, rather than offering precise site-specific predictions.

Materials and Methods

Study area

Kwara State, located in North-Central Nigeria (8°00'–9°30' N, 2°45'–6°40' E), spans approximately 36,825 km² and lies within the tropical wet-and-dry (Aw) climatic zone. Mean annual rainfall ranges from ~1,000 mm in the north to ~1,500 mm in the south, reflecting a distinct spatial gradient that influences rainfall erosivity (R-factor), a primary driver of soil detachment and runoff processes (Renard *et al.*,

2017). In tropical environments, such variability in precipitation is a key determinant of erosion intensity and spatial heterogeneity (Alemu *et al.*, 2026).

The state is predominantly covered by Guinea savanna vegetation, but extensive agricultural expansion and land-use conversion have resulted in fragmented vegetation cover. This modification directly affects the cover management factor (C-factor), as reduced canopy and ground cover increase soil exposure to rainfall impact and surface runoff (Panagos *et al.*, 2015). Land-use practices are largely characterized by rain-fed subsistence farming, often with limited soil conservation measures, thereby influencing the support practice factor (P-factor).

Soils in the region include Luvisols, Nitisols, Fluvisols, and Lithosols, with varying physical and chemical properties that determine their susceptibility to erosion. Differences in texture, structure, and organic matter content are reflected in the soil erodibility factor (K-factor), which governs the resistance of soil to detachment and transport (Borrelli *et al.*, 2017). Sandy and weakly structured soils are particularly vulnerable under high-intensity rainfall conditions typical of the region.

Topographically, Kwara State exhibits gently undulating terrain with localized areas of moderate to steep slopes, especially in the southeastern region. These variations influence runoff accumulation and flow velocity, represented in the slope length and steepness (LS-factor), which has been identified as a critical control on erosion magnitude in spatial modelling studies (Ganasri & Ramesh, 2016).

The interaction of rainfall variability, soil heterogeneity, land-use pressure, and topographic gradients creates a spatially diverse erosion landscape. These characteristics align directly with the input parameters of the RUSLE model (R, K, LS, C, and P), thereby providing a suitable basis for evaluating the relative distribution of soil erosion risk across the state within a GIS-based framework. Figure 1 presents a map of the study area.

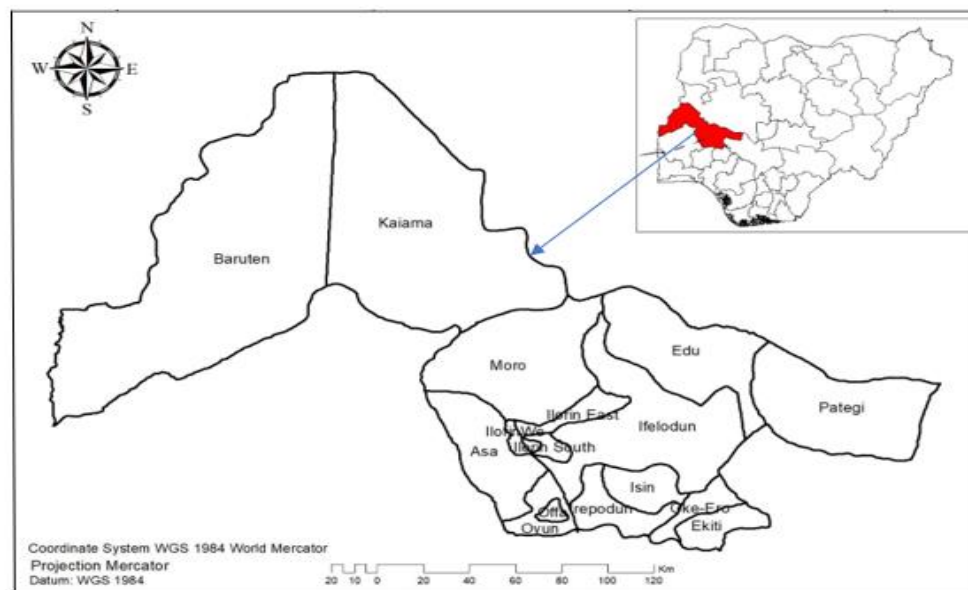


Figure 1: Map of the Study Area - top right; map of Nigeria; and bottom, map of Kwara State

Data sets and sources

This study integrates multiple geospatial datasets to derive the RUSLE factors (R, K, LS, C, and P). The datasets differ in spatial resolution and temporal coverage; therefore, careful preprocessing and harmonization were undertaken to ensure consistency in analysis.

Rainfall data were obtained from the Climate Hazards Centre/CHRS data portal, covering 30 years (1992–2022). The dataset has an approximate spatial resolution of 0.05° (~5 km). Mean annual precipitation was computed and interpolated using the Inverse Distance Weighted (IDW) method to generate a continuous raster surface for estimating the rainfall erosivity (R-factor). Long-term rainfall data are commonly used in RUSLE applications where high-resolution rainfall intensity records are unavailable (Renard *et al.*, 2017).

Topographic data were derived from the Shuttle Radar Topography Mission (SRTM) Digital Elevation Model (DEM) at 30 m spatial resolution, obtained from the U.S. Geological Survey. The DEM was used to compute slope, flow direction, and flow accumulation layers required for deriving the slope length and steepness (LS-factor). SRTM DEM is widely applied in erosion modelling due to its balance between spatial resolution and regional coverage (Ganasri & Ramesh, 2016).

Soil data were sourced from the FAO Harmonized World Soil Database (HWSD), originally provided at a spatial resolution of approximately 1 km. Soil properties, including texture and organic carbon content, were extracted and used to compute the soil erodibility (K-factor). Although coarser than the DEM, HWSD remains a commonly used dataset for regional-scale erosion studies (Borrelli *et al.*, 2017). Land use/land cover data were derived from MODIS products via Google Earth Engine, with an original

spatial resolution of 250 m. The Normalized Difference Vegetation Index (NDVI) was computed and used to estimate the cover management factor (C-factor), reflecting vegetation density and seasonal variability (Panagos *et al.*, 2015).

To ensure spatial consistency, all datasets were projected to a common coordinate system (WGS 1984, UTM Zone 31N) and resampled to a uniform spatial resolution of 30 m, corresponding to the DEM grid. Resampling of coarser datasets (rainfall, soil, and NDVI) to finer resolution was performed using appropriate interpolation techniques. While this approach enables pixel-level integration of RUSLE factors, it may introduce uncertainty due to the downscaling of coarse-resolution data, potentially affecting the precision of localized soil loss estimates. Despite these limitations, the integration of multi-source datasets at a harmonized resolution provides a practical and widely adopted approach for regional-scale erosion modelling. The results should therefore be interpreted as indicative of spatial patterns of erosion risk rather than exact point-scale measurements.

RUSLE model framework

Soil erosion was estimated using the Revised Universal Soil Loss Equation (RUSLE), expressed as:

$$A = R \times K \times LS \times C \times P \text{ (Equation 1)}$$

where:

- A = average annual soil loss ($t \text{ ha}^{-1} \text{ yr}^{-1}$)
- R = rainfall erosivity factor
- K = soil erodibility factor
- LS = slope length and steepness factor
- C = cover management factor
- P = support practice factor

Each factor was derived spatially and integrated within a GIS environment to produce a soil loss map (Figure 7).

Rainfall erosivity (R factor)

Rainfall erosivity represents the erosive potential of rainfall and is ideally derived from rainfall intensity data (Renard *et al.*, 2017). Rainfall erosivity (R-factor) was estimated using a precipitation-based empirical model appropriate for tropical, data-scarce environments (Equation 2). This formulation ensures consistency with RUSLE units ($\text{MJ mm ha}^{-1} \text{h}^{-1} \text{yr}^{-1}$).

$$R = 0.5 \times P \quad (\text{Equation 2})$$

where P is the mean annual rainfall (mm). This formulation has been widely applied in tropical, data-scarce environments (Alemu *et al.*, 2026).

Rainfall data were interpolated using the Inverse Distance Weighted (IDW) method to generate a continuous surface (Figure 2). The resulting R-factor represents relative erosivity patterns rather than event-based rainfall dynamics. While this approach does not specifically incorporate rainfall intensity, it is considered suitable for regional-scale erosion assessment and should be interpreted as an approximation of relative erosivity rather than a precise measurement.

Soil erodibility (K factor)

The soil erodibility factor (K-factor) quantifies soil susceptibility to detachment and transport. It was derived from HWSD soil attributes using the EPIC formulation (Williams & Singh, 1995) (Equation 3), where soil texture fractions and organic carbon content determine erodibility. The full formulation accounts for particle size distribution and organic matter effects on soil resistance (Borrelli *et al.*, 2017). The K-factor was computed as:

$$K = f_{sand} \times f_{clay} \times f_{orgC} \times f_{silt} \quad (\text{Eq. 3})$$

where:

$$f_{sand} = 0.2 + 0.3 \exp [-0.0256 \cdot sand \cdot (1 - \frac{silt}{100})]$$

$$f_{clay} = \left(\frac{silt}{clay + silt} \right)^{0.3}$$

$$f_{orgC} = 1 - \frac{0.25 \cdot C}{C + \exp (3.72 - 2.95C)}$$

$$f_{silt} = 1$$

$$= \frac{0.7(1 - \frac{sand}{100})}{(1 - \frac{sand}{100}) + \exp [-5.51 + 22.9(1 - \frac{sand}{100})]}$$

and sand, silt, clay = percentage fractions of soil particles and C = organic carbon content (%).

This formulation accounts for the influence of soil particle size distribution and organic matter on erosion resistance. It is particularly suitable for large-scale applications where detailed field measurements are unavailable and has been widely used in global and regional erosion studies (Borrelli *et al.*, 2017). The K-factor was computed using raster-based operations to produce a spatial erodibility map (Figure 3).

Slope Length and Steepness (LS Factor)

The LS factor represents the influence of topography on erosion and was calculated using the Desmet and Govers (1996) formulation: (Equation 4).

$$LS = \left(\frac{FA \times r}{22.13} \right)^m \times \left(\frac{\sin \theta}{0.0896} \right)^n \quad (\text{Eq. 4})$$

where:

- FA = flow accumulation
- r = cell size (30 m)
- θ = slope angle (radians)
- $m = 0.5, n = 1.3$

DEM-derived slope, flow direction, and flow accumulation were computed using the D8 algorithm. No flow threshold was applied, preserving a continuous upslope contributing area.

However, LS values are sensitive to DEM resolution and flow accumulation, potentially producing high values in areas of flow convergence. These should be interpreted as relative indicators of topographic influence (Ganasri & Ramesh, 2016).

Cover management (C factor)

The cover management factor (C) represents the effect of vegetation cover and land management on soil erosion. In this study, C was derived from the Normalized Difference Vegetation Index (NDVI) obtained from MODIS imagery.

NDVI was computed as:

$$NDVI = \frac{NIR - RED}{NIR + RED} \quad (\text{Eq. 5})$$

The C-factor was then estimated using the exponential relationship proposed by Durigon *et al.* (2014):

$$C = \exp \left[-\alpha \left(\frac{NDVI}{\beta - NDVI} \right) \right] \quad (\text{Eq. 6})$$

where α and β are empirical constants (commonly $\alpha = 2, \beta = 1$).

The MODIS NDVI dataset has a native spatial resolution of 250 m and was resampled to 30 m using bilinear interpolation to match the resolution of the DEM and enable raster-based integration of RUSLE factors.

While this resampling facilitates spatial consistency, it does not increase the inherent spatial detail of the NDVI data and may introduce smoothing effects or artificial spatial patterns. Such downscaling can influence the spatial variability of the C-factor and, consequently, soil loss estimates at finer scales (Panagos *et al.*, 2015).

Therefore, the C-factor map should be interpreted as representing generalized vegetation patterns rather than fine-scale land cover variability. Thus, the C-factor reflects generalized land cover conditions (Figure 7).

Support practice (P factor)

The support practice factor (P) reflects the impact of soil conservation measures on reducing erosion by modifying runoff flow patterns. In this study, P values were assigned based on slope classes using established

relationships from the literature (Wischmeier & Smith, 1978; Renard *et al.*, 2017).

Due to the absence of spatially defined data on conservation practices across Kwara State, a slope-based proxy approach was adopted. This assumes that areas under steeper slopes are less likely to implement effective conservation practices, while gentler slopes may support practices such as contouring.

The P-factor values were assigned according to slope ranges and generalized conservation conditions. This approach has been widely used in regional-scale RUSLE applications where field-based conservation data are unavailable (Ganasri & Ramesh, 2016).

Table 1: P factor depending on cultivation types and slope

S/N	Slope	Contouring	Stripping	Terracing
1	0.0 -7.00	0.55	0.27	0.10
2	7.00 – 11.3	0.60	0.30	0.12
3	11.3 – 17.6	0.80	0.40	0.16
4	17.6 – 26.8	0.90	0.45	0.18
5	26.8 >	1.00	0.50	0.20

(Source: Korea Institute of Construction Technology, 1992).

Soil loss estimation and classification

All RUSLE factors (R, K, LS, C, and P) were integrated in ArcGIS using raster multiplication (Equation 1) to produce a spatial soil loss map (Figure 7). The maps were projected from Geographic Coordinate Projection (GCP) to WGS 1984, UTM zone 31, using the ArcGIS tool. The raster maps of the soil loss factors were integrated using the RUSLE relation to generate composite maps of the estimated soil loss, which summed to produce the final variability map of the study area. The resulting map was reclassified into three classes (low, medium, and high) using the reclassify software package in ArcGIS before the final map production.

Accuracy assessment

The accuracy of the soil erosion classification was evaluated using an independent set of ground-referenced observations and a confusion matrix approach (Foody, 2024). A total of 59 validation points were selected using stratified random sampling to ensure representation across erosion classes and spatial variability within the study area. These points were independent of model input datasets.

However, it is acknowledged that agricultural practices in Kwara State are predominantly smallholder and heterogeneous, and the actual implementation of conservation measures may vary significantly across locations. As such, the assigned P values represent generalized conditions and introduce uncertainty into the model. The P-factor should therefore be interpreted as an approximation of support practice influence rather than a direct representation of site-specific conservation measures. Table 1 presents the P factor depending on the cultivation types and slope.

Overall accuracy, producer accuracy, user accuracy, and the kappa coefficient were computed from the confusion matrix. The results (Table 2) indicate an overall accuracy of 93% and a kappa coefficient of 0.87, suggesting strong agreement beyond chance.

However, given the limited sample size, these metrics should be interpreted with caution. Approximate confidence intervals based on binomial assumptions indicate potential variability in the reported accuracy, particularly at the class level. Inconsistencies in earlier kappa reporting have been corrected to ensure internal consistency. The validation provides indicative rather than definitive accuracy, and future work should incorporate larger, more spatially distributed samples and uncertainty analysis to improve robustness.

The Kappa coefficient value is calculated as follows:

$$K = \frac{N \sum_{i=1}^r x_{ii} - \sum_{i=1}^r (x_i + x_{+i})}{N^2 - \sum_{i=1}^r (x_i + x_{+i})} \quad (\text{Eq. 7})$$

where r is the number of rows in the matrix, x_{ii} is the number of observations in row i and column i, x_{i+} and x_{+i} are the marginal total of row i and column i, and N is the total number of observations.

Table 2: Accuracy Assessment

Class Value	Low	Medium	High	Total	User Accuracy	Kappa
Low	37	0	0	37	1	0
Medium	3	9	0	12	0.75	0
High	1	0	9	10	0.9	0
Total	41	9	9	59	0	0
Producer Accuracy	0.902439	1	1	0	0.932203	0
Kappa	0	0	0	0	0	0.866365

Results

Spatial structure of erosion drivers

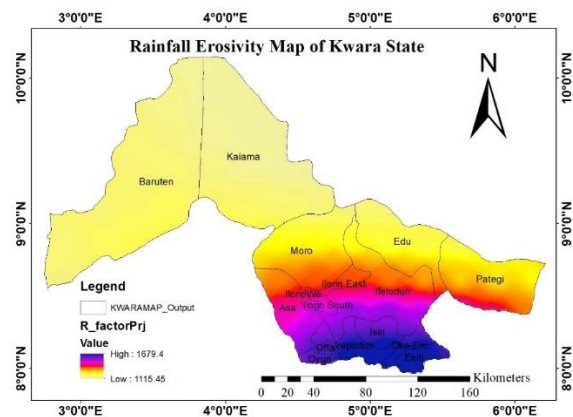


Figure 2: Rainfall Erosivity Map

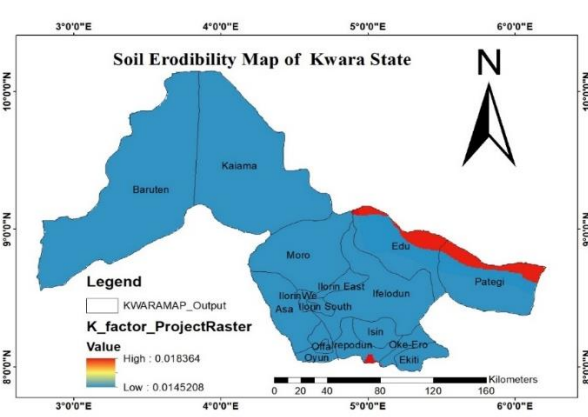


Figure 3: Soil Erodibility Map

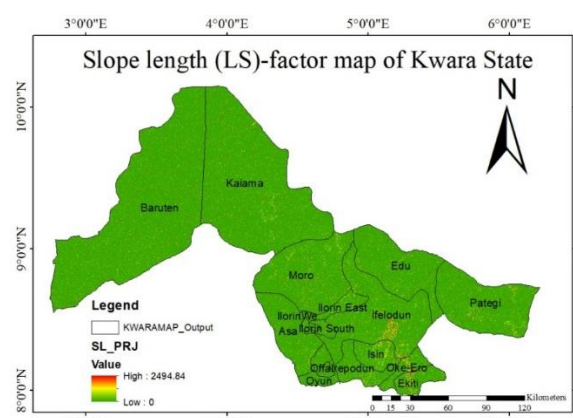


Figure 4: Slope Length (LS) factor Map

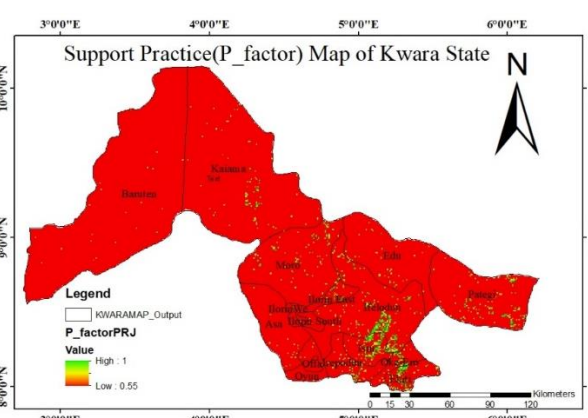


Figure 5: Support factor (P factor) Map

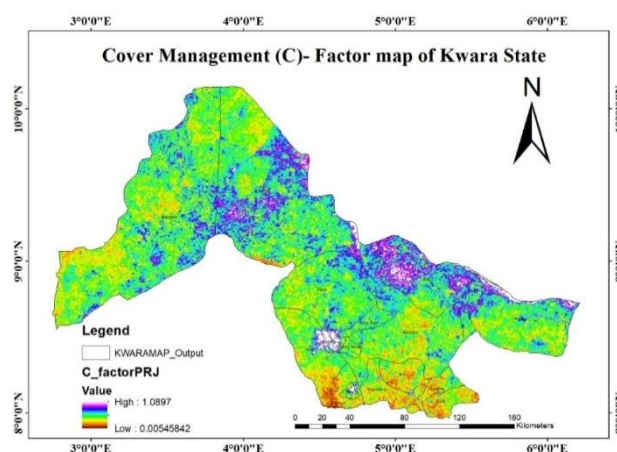


Figure 6: Cover management factor (C factor) Map

The spatial distribution of RUSLE factors (Figures 3–6) reveal a non-uniform erosion system driven by interacting climatic, topographic, and land-use controls. Rainfall erosivity (R-factor) increases from approximately 1115 to 1679 MJ mm ha⁻¹ h⁻¹ yr⁻¹ toward the southern LGAs, including Isin, Offa, Oke-Ero, and Ekiti (Figure 2). This gradient aligns with

observed rainfall patterns and establishes a primary climatic control on erosion potential. However, R alone does not explain the spatial distribution of soil loss. High R values in southern LGAs do not uniformly correspond to the highest erosion rates, indicating that rainfall influence is moderated by other factors. For instance, parts of Oyun and Irepodun, despite high R values, exhibit

moderate erosion due to relatively lower LS values and improved vegetation cover (Figure 6).

The LS factor (Figure 4) exhibits the strongest spatial contrast, with extreme values (up to ~2494) concentrated in the southeastern highlands and river-adjacent zones. These areas correspond to LGAs such as Ekiti, Oke-Ero, and Ifelodun, where slope gradients and flow accumulation combine to increase runoff energy. However, the magnitude of LS values is notably higher than typical ranges reported in comparable studies, suggesting sensitivity to DEM resolution and flow accumulation modelling (Desmet & Govers, 1996). This highlights a key methodological limitation, where topographic amplification may overestimate erosion potential in localized zones.

The C-factor (Figure 6) further differentiates erosion risk spatially. Low C values (<0.01) dominate forested and grassland areas in Oyun and Irepodun, whereas higher values (>1.0) occur in intensively cultivated or disturbed areas such as Edu, Baruten, and Ilorin West. This contrast demonstrates that vegetation cover acts as a critical moderating factor, often offsetting high topographic or rainfall-driven erosion potential.

Soil erodibility (K-factor) shows relatively limited variability (Figure 3), with values ranging narrowly (~0.0145–0.0184 t ha h ha⁻¹ MJ⁻¹ mm⁻¹). Higher K values in Edu, Patégi, and parts of Irepodun correspond to Fluvisols and Lithosols, which are

structurally weaker. However, these areas do not consistently align with the highest erosion rates, reinforcing that K plays a secondary, modifying role relative to LS and C.

Spatial patterns of soil loss

The integrated soil loss map (Figure 7) indicates that 73.15% (2.52 million ha) of the study area falls within the low erosion class, 23.04% (0.79 million ha) within the medium class, and only 3.81% (0.13 million ha) within the high-risk category (Table 3). This distribution suggests that erosion risk is spatially concentrated rather than uniformly distributed.

High-risk zones are localized in LGAs such as Ilorin South, Isin, Ifelodun, Oke-Ero, and Ekiti, where multiple high-impact factors converge, including elevated rainfall erosivity, steep slopes with high LS values, reduced vegetation cover, and limited conservation practices.

Conversely, northern LGAs such as Baruten and Kaiama, despite having areas of disturbed land cover, remain largely within the low-risk category due to lower rainfall and gentler slopes.

The soil loss distribution is highly skewed, with a small proportion of the landscape contributing disproportionately to total erosion. This pattern is consistent with erosion dynamics in tropical environments, where localized hotspots dominate sediment production (Alemu *et al.*, 2026).

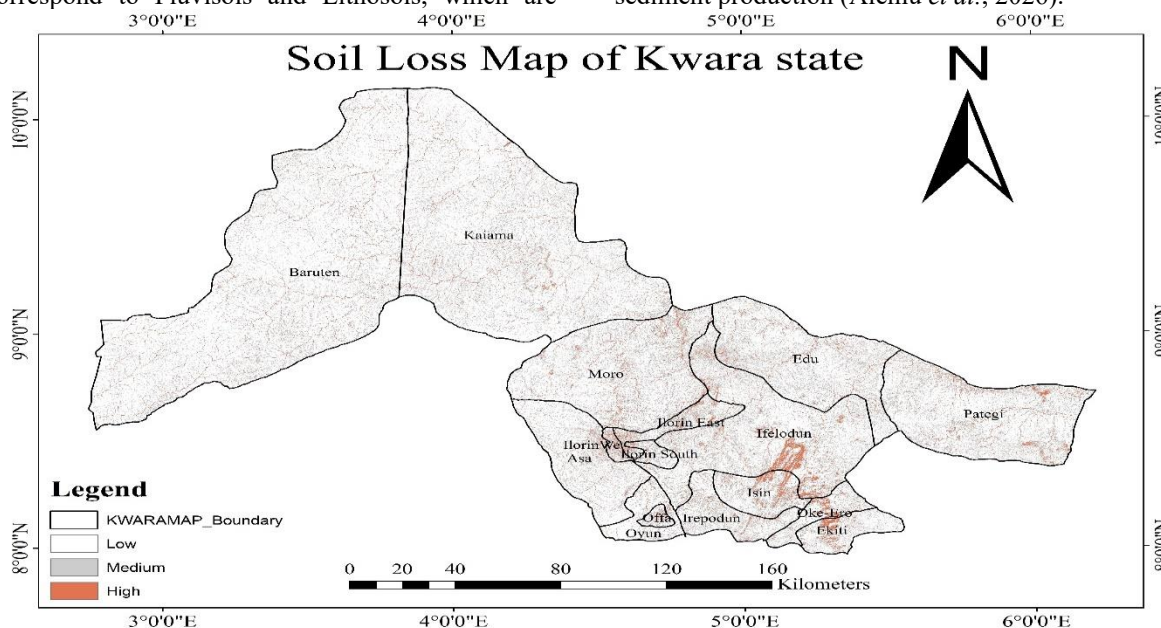


Figure 7: Soil Loss Map of Kwara State

Table 3: Annual Soil Loss of Kwara State

Vulnerability level	Percentage (%)	Area (Hectares)
Low	73.151232	2522328.48
Medium	23.043085	794548.89
High	3.805683	131223.78

Discussion

The results demonstrate that topography (LS) and vegetation cover (C) exert the strongest controls on erosion patterns, while rainfall (R) provides a background climatic driver. High erosion zones consistently occur where high LS values coincide with high C values, indicating exposed slopes with significant runoff accumulation.

For example, in Oke-Ero and Ekiti LGAs, the co-occurrence of steep slopes and sparse vegetation produces disproportionately high erosion estimates, even where soil erodibility is moderate. In contrast, areas with similar LS values but lower C values (denser vegetation) show reduced erosion, confirming the mitigating effect of vegetation.

The P-factor shows limited spatial differentiation due to its generalized assignment, but it contributes to increased erosion estimates in areas lacking conservation practices. However, its influence is secondary compared to LS and C, consistent with findings from other RUSLE-based studies (Ganasri & Ramesh, 2016).

The dominance of topography and vegetation in controlling erosion aligns with previous studies in tropical and sub-Saharan environments (Alemu *et al.*, 2026; Kayet *et al.*, 2018). However, the relatively low proportion of high-risk areas (3.81%) contrasts with studies in more mountainous or degraded regions, where higher erosion extents are reported.

These differences can be attributed to topographic variability, as Kwara State exhibits moderate relief compared to more highly dissected terrains; rainfall representation, where the use of mean annual rainfall may underestimate localized high-intensity events; and data resolution effects, since the resampling of coarse datasets such as NDVI and soil data can smooth out important spatial variability.

Additionally, the unusually high LS values observed in this study suggest potential overestimation due to flow accumulation sensitivity, a limitation also noted in similar GIS-based RUSLE applications (Desmet & Govers, 1996).

Several factors influence the magnitude and spatial distribution of predicted soil loss, including rainfall representation, where the use of mean annual rainfall fails to capture rainfall intensity and may underestimate erosivity under convective storm conditions; topographic sensitivity, as LS values depend strongly on DEM resolution and flow accumulation modelling, potentially exaggerating erosion in convergence zones; data resampling, since downscaling NDVI (250 m to 30 m) and soil data (approximately 1 km to 30 m) introduces spatial generalization; P-factor generalization, because slope-based estimates do not adequately reflect actual conservation practices across LGAs; and validation limitations, given that the relatively small validation sample (Table 5) restricts confidence in classification accuracy. These limitations indicate that the results should be interpreted as representing relative erosion

susceptibility patterns rather than absolute soil loss estimates.

The concentration of high erosion risk within a relatively small proportion of the landscape suggests that targeted intervention strategies are likely to be more effective than uniform approaches. Priority areas include LGAs such as Isin, Ifelodun, Oke-Ero, and Ekiti, where multiple risk factors converge. Management efforts should therefore focus on improving vegetation cover in high C-factor zones, reducing slope length through appropriate land management practices, and implementing localized conservation measures. However, given the methodological constraints, these recommendations should be regarded as indicative spatial priorities rather than prescriptive interventions.

The RUSLE model does not account for gully erosion, sediment deposition, or rainfall intensity variability. Additionally, resampled datasets and generalized P-factor assumptions introduce uncertainty. Therefore, results represent relative erosion susceptibility rather than absolute soil loss estimates.

Conclusion

This study applied the RUSLE model integrated with GIS and remote sensing techniques to assess the spatial variability of soil erosion in Kwara State, Nigeria. The results provide a spatially defined estimate of average annual soil loss based on rainfall erosivity, soil erodibility, topography, vegetation cover, and support practices.

The findings indicate that much of the study area falls within the low-erosion-risk category (73.15%). In comparison, moderate (23.04%) and high-risk areas (3.81%) are spatially concentrated in specific locations, particularly along river channels, cultivated lands, and areas with sparse vegetation cover. These patterns reflect the combined influence of rainfall intensity, slope characteristics, and land cover conditions.

The results highlight priority areas where soil conservation measures may be most needed, particularly in parts of Ilorin, Isin, Ifelodun, Oke-Ero, Ekiti, and Offa. However, these findings should be interpreted as indicative of relative erosion susceptibility rather than precise predictions of soil loss magnitudes. It is important to note that the RUSLE model is an empirical approach that does not clearly account for gully erosion, sediment deposition, or event-based dynamics. In addition, the validation was based on a limited number of ground-truth observations, and no sensitivity or uncertainty analysis was conducted. As such, the results should be interpreted with caution.

Future studies should incorporate higher-resolution rainfall-intensity data, expand field-based validation, and include uncertainty- or scenario-based analyses to strengthen the robustness of erosion assessments. Despite these limitations, the study provides a useful baseline for identifying erosion-prone areas and

supporting targeted land management interventions within the study area.

Conflict of Interest

The authors declare the absence of conflict of interest.

References

- Alemu, M. D., Aweke, A., Van Tol, J., & Mengistu, A. G. (2026). Spatio-temporal modeling of soil erosion dynamics under land use and land cover changes in the Bilate river catchment, Ethiopia. *Environmental Earth Sciences*, 85(1), 3. <https://doi.org/10.1007/s12665-025-12709-z>
- Anejionu, C. D. O., Blackburn, G. A., & Whyatt, J. D. (2013). Detecting gas flares and estimating flared gas volumes using Landsat data in Nigeria. *Remote Sensing*, 5(9), 4305–4322. <https://doi.org/10.1016/j.rse.2014.11.018>
- Boardman, J., & Poesen, J. (2006). Soil erosion in Europe: Major processes, causes and consequences. *Geomorphology*, 79(1–2), 1–3. <https://doi.org/10.1002/0470859202.ch36>
- Borrelli, P., Robinson, D. A., Fleischer, L. R., Lugato, E., Ballabio, C., Alewell, C., ... & Panagos, P. (2017). An assessment of the global impact of 21st-century land use change on soil erosion. *Nature communications*, 8(1), 2013. <https://doi.org/10.1038/s41467-017-02142-7>
- Desmet, P. J. J., & Govers, G. (1996). A GIS procedure for automatically calculating the USLE LS factor on topographically complex landscape units. *Journal of Soil and Water Conservation*, 51(5), 427–433. <https://doi.org/10.1080/00224561.1996.12457102>
- Durigon, V. L., Carvalho, D. F., Antunes, M. A. H., Oliveira, P. T. S., & Fernandes, M. M. (2014). NDVI time series for C-factor estimation in RUSLE. *Geoderma*, 226–227, 239–248. <https://doi.org/10.1016/j.geoderma.2014.02.024>
- Foody, G. M. (2024). Ground truth in classification accuracy assessment: myth and reality. *Geomatics*, 4(1), 81–90. <https://doi.org/10.3390/geomatics4010005>
- Ganasri, B. P., & Ramesh, H. (2016). Assessment of soil erosion by RUSLE model using remote sensing and GIS: A case study of Nethravathi Basin. *Geoscience Frontiers*, 7(6), 953–961. <https://doi.org/10.1016/j.gsf.2015.10.007>
- Kayet, N., Pathak, K., Chakrabarty, A., & Sahoo, S. (2018). Evaluation of soil loss estimation using the RUSLE model and geospatial techniques. *Modeling Earth Systems and Environment*, 4, 893–905. <https://doi.org/10.1016/j.iswcr.2017.11.002>
- Panagos, P., Borrelli, P., Meusburger, K., Alewell, C., Lugato, E., & Montanarella, L. (2015). Estimating the soil erosion cover-management factor at the European scale. *Land Use Policy*, 48, 38–50. <https://doi.org/10.1016/j.landusepol.2015.05.021>
- Poesen, J. (2018). Soil erosion in the Anthropocene: Research needs. *Earth Surface Processes and Landforms*, 43(1), 4–16. <https://doi.org/10.1002/esp.4250>
- Renard, K. G., Laflen, J. M., Foster, G. R., & McCool, D. K. (2017). The revised universal soil loss equation. In *Soil erosion research methods* (pp. 105–126). Routledge. <https://doi.org/10.1201/9780203739358-5>
- Tamene, L., & Vlek, P. L. G. (2008). Soil erosion studies in Sub-Saharan Africa: A review. *Land Use Policy*, 25(4), 547–560. https://doi.org/10.1007/978-1-4020-6778-5_5
- Thapa, P. (2020). Spatial estimation of soil erosion using RUSLE modeling. *Environmental Systems Research*, 9(1). <https://doi.org/10.1186/s40068-020-00177-2>
- Williams & Singh, J. R., & Singh, V. (1995). The EPIC model. Computer models of watershed hydrology. *Water Resour. Publ. Highl. Ranch Colo*, 25, 909–1000.
- Wischmeier, W. H., & Smith, D. D. (1978). *Predicting rainfall erosion losses: a guide to conservation planning* (No. 537). Department of Agriculture, Science and Education Administration.